

# Photoacoustic characterization of the effects of air inclusion on the thermal properties of foamed polyurethane

N. F. LEITE

*Laboratório Associado de Sensores e Materiais, Instituto de Pesquisas Espaciais, Caixa Postal 515, 12201 – São José dos Campos, S.P., Brazil*

L. C. M. MIRANDA\*

*Instituto Politécnico do Rio de Janeiro, Caixa Postal 97282, 28600 – Nova Friburgo, R.J., Brazil*

The usefulness of the open photoacoustic cell technique for investigating the effects of air inclusions on the thermal properties of foamed polyurethane is demonstrated. It is shown that the thermal diffusivity and thermal expansion coefficients increase with decreasing values of the resin to catalyst ratio, which corresponds to greater air inclusion in the resin.

## 1. Introduction

In the last decade, several methods have been developed to determine thermal properties with high precision by means of photothermal effects (for a review, see [1]). The most widely used method is based upon the photoacoustic (PA) effect. The PA effect involves the heat generated in a sample, due to non-radiative de-excitation processes, following the absorption of light. In the conventional experimental arrangement, a sample is enclosed in an air-tight cell and exposed to a chopped light beam. As a result of the periodic heating of the sample, the pressure in the cell oscillates at the chopping frequency and can be detected by a sensitive microphone coupled to the cell. The resulting signal depends not only on the amount of heat generated in the sample (and, hence on the optical absorption coefficient and the light-into-heat conversion efficiency of the sample), but also on how the heat diffuses through the sample. The quantity which measures the rate of heat diffusion is the thermal diffusivity,  $\alpha$

$$\alpha = \frac{k}{\rho c} \quad (1)$$

where  $k$  is the thermal conductivity,  $\rho$  is the density, and  $c$  is the specific heat at constant pressure. Apart from interest in its intrinsic value, the importance of  $\alpha$  as a physical parameter to be monitored is due to the fact that, like the optical absorption coefficient, it is unique for each material. This can be appreciated by the tabulated values of  $\alpha$  given by Touloukian *et al.* [2] for a wide range of materials, such as metals, minerals, foodstuffs, biological specimens and polymers. Furthermore, the thermal diffusivity is also known to be extremely dependent on the effects of

compositional and microstructural variables [3], such as processing conditions, as in the cases of polymers [4–8], ceramics [3] and glasses [9].

The PA effect has been proved by several authors [10–14] to be a simple and reliable technique for measuring the thermal properties of solid samples. In the present work, we applied the recently proposed open photoacoustic cell (OPC) [15, 16] in order to investigate the effects of air inclusions on the thermal properties of foamed polyurethane.

## 2. Experimental procedure

The samples investigated were prepared using different compositions of polyurethane resin (Solithane 113, Thiokol Chemicals) and catalyst (C113 polyalcohol, Thiokol Chemicals). The samples were prepared on a clean glass plate by mixing drops of resin (R) and catalyst (C) at different R/C ratios. After thoroughly stirring, the samples were spread on one face of a 6 mm diameter aluminium disc 60  $\mu\text{m}$  thick, and left to cure for about 5 days. The OPC experimental arrangement is shown schematically in Fig. 1. It consists of a 250 W halogen-tungsten lamp whose polychromatic beam is mechanically chopped and focused on to the uncoated aluminium face of the sample. The sample is mounted directly on to a circular electret microphone. The typical design of an electret microphone [17] consists of a metalized electric diaphragm (12  $\mu\text{m}$  fluoroethylene propylene with a 50–100 nm thick deposited metal electrode) and a metal back plate separated from the diaphragm by an air gap (45  $\mu\text{m}$  wide). The metal layer and back plate are connected through a resistor,  $R$ . The front sound inlet is a circular hole, 3 mm diameter, and the front air

\*Permanent address: Instituto de Pesquisas Espaciais, S.J. Campos, S.P., Brazil.

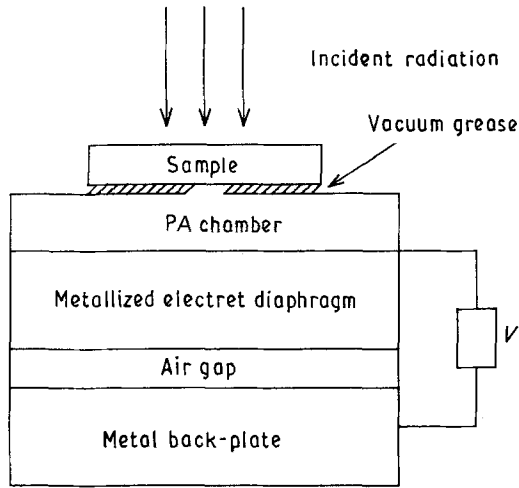


Figure 1 Cross-section of the open photoacoustic cell using the front air chamber of a common electret microphone as a transducer medium.

chamber adjacent to the metalized face of the diaphragm is roughly 1 mm long. As a result of the periodic heating of the sample by the absorption of modulated light, the pressure in the front chamber oscillates at the chopping frequency, causing diaphragm deflections, which generate a voltage,  $V$ , across the resistor. This output voltage from the microphone is connected to a lock-in amplifier in which the signal amplitude and phase are both recorded as a function of the modulation frequency. The use of the 60  $\mu\text{m}$  aluminium discs to support the samples ensures that the heat deposited is the same for all samples and that it is essentially instantaneously transmitted to the outer face of the samples. We note that for a 60  $\mu\text{m}$  thick aluminium foil the heat diffusion time ( $\sim l^2/\alpha$ ) is roughly 39  $\mu\text{s}$  which is much shorter than that of a typical 100  $\mu\text{m}$  thick polyurethane sample (of the order of 90 ms).

The output voltage,  $V$ , is obtained from the so-called kettledrum model [17] for the electret microphone and is proportional to the pressure fluctuation in the front air chamber. This, in turn, is given by the composite thermal piston model [18, 19] according to which the total pressure fluctuation in the PA cell is due to three main contributions: (i) sample to gas thermal diffusion, which is sensitive to the sample surface temperature as described by the Rosenzweig and Gersho model [20]; (ii) sample thermal expansion which depends on the average sample temperature; and (iii) thermoelastic bending which is essentially due to the temperature gradient inside the sample along the thickness axis ( $x$ -axis). Owing to the existence of this temperature gradient along the  $x$ -axis, the thermal expansion depends on  $x$ . This entails in an  $x$ -dependence of the sample displacement along the radial direction thereby inducing a bending of the sample in the  $x$  direction. The contribution from the sample bending and dilation is formally described by the coupled set of thermoelastic equations and is described in detail elsewhere [16, 21]. It can be shown [16, 21] that for samples with the lateral dimension much greater than the thickness, the thermoelastic bending is the dominant contribution to the vibrating sample piston. Assuming an optically opaque sample,

which is appropriate for our aluminium-supported sample (the uncoated aluminium surface facing the light beam), and solving the thermal diffusion and thermoelastic equations as detailed elsewhere [16, 21], the output voltage can be written as

$$V = V_0 \frac{j\omega\tau_E}{(1 + j\omega\tau_E)} \frac{\beta I_0 e^{j\omega t}}{T_0 l_g \sigma_g k_s \sigma_s} \left\{ \frac{[1 - e^{-(l_g \sigma_g)}]}{\sinh(l_s a_s)} - \frac{3R_0^4 \alpha_T T_0 \alpha_s^{1/2}}{2R_c^2 l_s^2 \alpha_g^{1/2}} \times \frac{[l_s \sigma_s \sinh(l_s \sigma_s) - \cosh(l_s \sigma_s) + 1]}{l_s \sigma_s \sinh(l_s \sigma_s)} \right\} \quad (2)$$

where  $T_0$  is the ambient temperature,  $I_0$  is the incident light intensity at a given wavelength,  $\beta$  is the surface absorption coefficient,  $V_0 = (l_b l_m \sigma_0)/(l_b \epsilon + l_m \epsilon_0)$ , where  $\sigma_0$  is the charge density per  $\text{cm}^2$ ,  $\epsilon$  the dielectric constant,  $l_b$  the static back plate air gap thickness and  $l_m$  the electret membrane thickness.  $\tau_E$  is the electronic time constant,  $l_i$ ,  $k_i$  and  $\alpha_i$  are the length, thermal conductivity and thermal diffusivity of material  $i$ . Here the subscript  $i$  denotes the sample(s) and gas(g), respectively, and  $\sigma_i = (1 + j)a_i$ , with  $a_i = (\pi f/\alpha_i)^{1/2}$  being the thermal diffusion coefficient of material  $i$ ,  $R_c$  is the radius of the PA chamber in front of the microphone diaphragm ( $R_c = 3.5$  mm),  $R_0$  is the support radius of the sample (i.e. the radius of the microphone front hole,  $R_0 = 1.5$  mm) and  $\alpha_T$  is the sample thermal expansion coefficient. The first term in Equation 2 is due to the air contribution whereas the second one represents the sample thermal expansion contribution.

The thermal diffusivity and expansion coefficient are obtained by fitting the experimental data to Equation 2 leaving  $\alpha_s$  and  $\alpha_T$  as adjustable parameters. Fig. 2 shows the OPC signal amplitude data as a function of the modulation frequency for the sample having a R/C ratio equal to 1.33, prepared using four drops of resin to three drops of catalyst. The solid line in Fig. 2 corresponds to the best fit of the data to the theoretical expression for the OPC signal amplitude obtained from Equation 2. Table I summarizes the

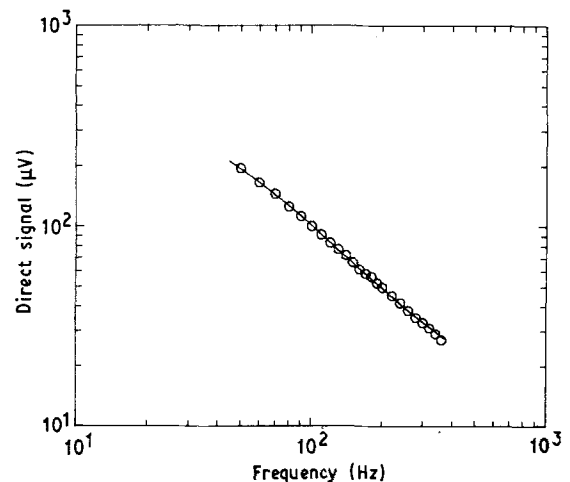


Figure 2 Opac signal amplitude as a function of the modulation frequency for a sample prepared using four drops of polyurethane resin and three drops of catalyst. Data fitting to Equation 2.

values of  $\alpha_s$  and  $\alpha_T$  obtained from this procedure for the samples studied. The samples are denoted by two digits where the first one denotes the number of resin drops and the second one denotes the number of catalyst drops used in their preparation.

### 3. Discussion and conclusion

Fig. 3 shows the thermal diffusivity and thermal expansion coefficient data, as given in Table I, as a function of the ratio R/C. We note from Fig. 3 that for large values of R/C both  $\alpha_s$  and  $\alpha_T$  tend to be equal to the corresponding values of the polyurethane resin,  $\alpha_s = 0.0011 \text{ cm}^2 \text{ s}^{-1}$  and  $\alpha_T = 1.2 \times 10^{-4} \text{ K}^{-1}$ , as given by the manufacturer's data sheet. For small values of R/C, the values of the thermal diffusivity and thermal expansion coefficient increases with decreasing values of R/C. We attribute this behaviour of  $\alpha_s$  and  $\alpha_T$  to the presence of air inclusions. In fact, for large R/C values, the samples have a small number

$$\alpha = \alpha_1 \frac{2(1-x) + (1+2x)\lambda}{[2+x+(1-x)\lambda][1-x+x(\rho_2 c_2 / \rho_1 c_1)]} \quad (5)$$

of air bubbles and look like the bare resin. Noting that the values of  $\alpha_s$  and  $\alpha_T$  for air (namely,  $\alpha_s = 0.21 \text{ cm}^2 \text{ s}^{-1}$ ,  $\alpha_T = 0.0033 \text{ K}^{-1}$ ) are much greater than those for the polyurethane resin, one would then expect that the thermal diffusivity and the expansion

TABLE I Values of the resin to catalyst ratio, thermal diffusivity and thermal expansion coefficients for the foamed polyurethane samples. The samples are denoted by two digits. The first one refers to the number of resin drops used in the preparation whereas the second one refers to the number of catalyst drops.

Sample	R/C	$\alpha_s (\text{cm}^2 \text{ s}^{-1})$	$\alpha_T (10^4 \text{ K}^{-1})$
51	5	0.0019	1.7
41	4	0.00226	2.3
42	2	0.00219	1.5
43	1.33	0.0181	6.7
33	1	0.0241	8.3
52	2.5	0.0303	12.2

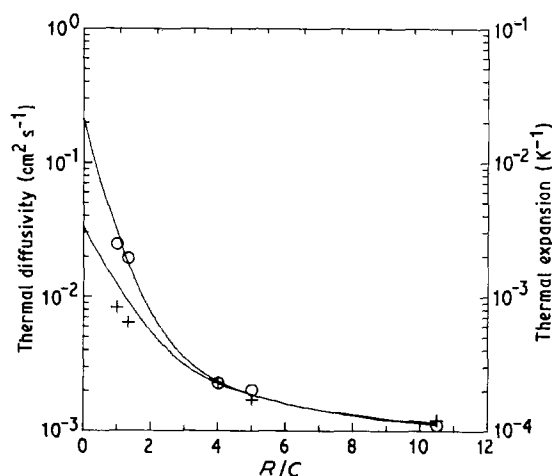


Figure 3 (○) Thermal diffusivity and (×) thermal expansion coefficient as a function of the resin to catalyst ratio used in the sample preparation.

coefficient would increase with decreasing R/C ratio.

This expectation may be quantitatively described assuming the Maxwell-Rayleigh model [22, 23] for the foamed samples. This model consists of randomly dispersed spherical particles (representing the air inclusions), labelled subscript 2, embedded in a continuous medium (representing the resin), labelled subscript 1. The Maxwell-Rayleigh relation for the effective thermal conductivity is given by

$$k = k_1 \frac{2(1-x) + (1+2x)\lambda}{2+x+(1-x)\lambda} \quad (3)$$

where  $\lambda = k_2/k_1$  and  $x$  is the volume fraction of the dispersed particles (i.e. the air inclusion volume fraction). On the other hand, the effective heat capacity,  $v\rho c$ , of the composite sample is given by

$$v\rho c = v_1\rho_1c_1 + v_2\rho_2c_2 \quad (4)$$

Substituting Equations 3 and 4 into Equation 1, the thermal diffusivity of the composite samples is written as

Fig. 4 shows the dependence of  $\alpha$  given by Equation 5 on the volume fraction  $x$ . Known values for the resin and air thermal properties have been used, namely,  $\alpha_1 = 0.0011 \text{ cm}^2 \text{ s}^{-1}$ ,  $k_1 = 2.1 \text{ mW cm}^{-1} \text{ K}^{-1}$ ,  $\alpha_{T1} = 1.2 \times 10^{-4} \text{ K}^{-1}$ ,  $\alpha_2 = 0.21 \text{ cm}^2 \text{ s}^{-1}$ ,  $k_2 = 0.26 \text{ mW cm}^{-1} \text{ K}^{-1}$ ,  $\alpha_{T2} = 33.3 \times 10^{-4} \text{ K}^{-1}$ . We note from Fig. 4 that up to  $x = 0.70$  the thermal diffusivity is essentially that of the resin. For larger air inclusion content, the thermal diffusivity increases quite sharply with increasing  $x$ . The effective thermal expansion coefficient,  $\alpha_T$ , for this composite sample is obtained from the above model, as follows. From Equation 4

$$\delta l \rho c = \delta l_1 \rho_1 c_1 + \delta l_2 \rho_2 c_2 \quad (6)$$

Writing  $\delta l = \alpha_T l \delta T$  and  $\delta l_i = \alpha_{Ti} l_i \delta T$  gives

$$\alpha_T = \frac{\alpha_{T1} \rho_1 c_1 (1-x) + \alpha_{T2} \rho_2 c_2 x}{(1-x)\rho_1 c_1 + x\rho_2 c_2} \quad (7)$$

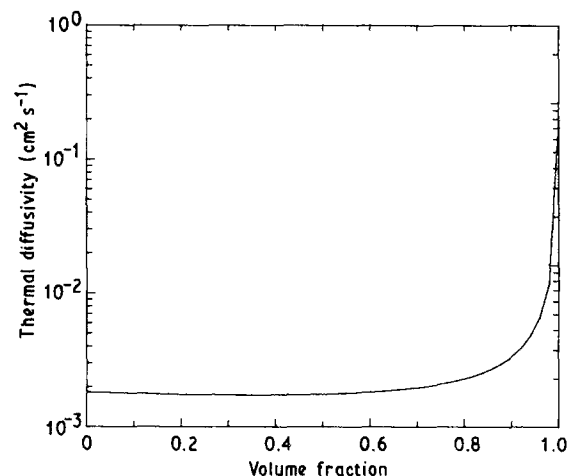


Figure 4 Dependence of the thermal diffusivity of foamed polyurethane as a function of the air volume content,  $x$ , as predicted by Equation 5.

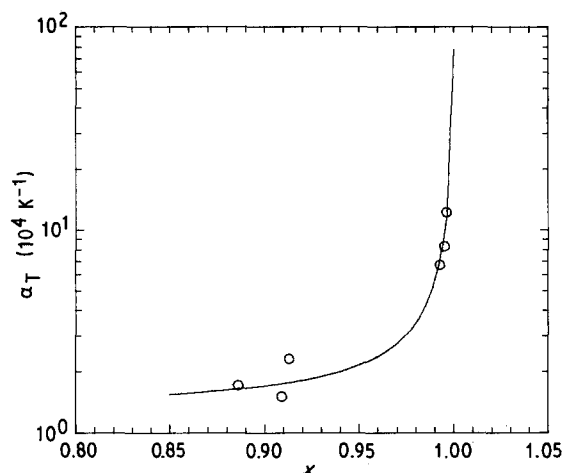


Figure 5 Thermal expansion coefficient as a function of the air volume content,  $x$ . (—) The best fit of the data to Equation 7.

As a quantitative check on this model for our foamed samples we proceeded as follows. Using the known values of the thermal properties for the air and resin, together with the experimental data obtained for the thermal diffusivity, we used Equation 5 to determine the volume fractions for the samples studied. This value of  $x$  and the experimental data for  $\alpha_T$  were then used to find the thermal expansion coefficients,  $\alpha_{T1}$  and  $\alpha_{T2}$ , as well as the specific heat ratio,  $\rho_2 c_2 / \rho_1 c_1$ , from the data fitting to Equation 7. Fig. 5 shows the thermal expansion coefficient data as a function of the volume fraction  $x$ , obtained from the thermal diffusivity values, as described above. The solid line in Fig. 5 represents the best fit of the data to the theoretical expression for  $\alpha_T$  given by Equation 7. The results obtained from the fitting procedure were  $\alpha_{T1} = 1.2 \times 10^{-4} \text{ K}^{-1}$ ,  $\alpha_{T2} = 48 \times 10^{-4} \text{ K}^{-1}$ ,  $\rho_2 c_2 / \rho_1 c_1 = 0.0006$ . From this value of the specific heat ratio, using the resin value,  $\rho_1 c_1 = 1.926 \text{ J cm}^{-3} \text{ K}^{-1}$ , we find  $\rho_2 c_2 = 0.0012 \text{ J cm}^{-3} \text{ K}^{-1}$  for the air specific heat, which agrees very well with the literature value. The air thermal expansion coefficient was found to be larger than expected. This discrepancy may be due to the fact that the bubbles may not be filled only with air but rather with a mixture of air and vapour products from the resin-catalyst reaction.

In conclusion, the usefulness of the OPC technique

for investigating the thermal properties of solid samples has been demonstrated.

## References

1. H. VARGAS and L. C. M. MIRANDA, *Phys. Rep.* **161** (1988) 43.
2. Y. S. TOULOUKIAN, R. W. POWELL, C. Y. HO and M. C. NICOLASU, in "Thermal Diffusivity" (IFI/Plenum, New York, 1973).
3. G. ZIEGLER and D. P. H. HASSELMAN, *J. Mater. Sci.* **16** (1981) 495.
4. N. F. LEITE, N. CELLA, H. VARGAS and L. C. M. MIRANDA, *J. Appl. Phys.* **61** (1987) 3023.
5. A. TORRES-FILHO, L. F. PERONDI and L. C. M. MIRANDA, *J. Appl. Polym. Sci.* **35** (1988) 103.
6. B. MERTÉ, P. KORPIUN, E. LÜSHER and R. TILGNER, *J. Phys. Coll.* **44** (1983) 463.
7. A. TORRES-FILHO, N. F. LEITE, L. C. M. MIRANDA, N. CELLA and H. VARGAS, *J. Appl. Phys.* **66** (1989) 97.
8. A. H. FRANZAN, N. F. LEITE and L. C. M. MIRANDA, *Appl. Phys. A* **50** (1990) 431.
9. A. C. BENTO, H. VARGAS, M. M. F. AGUIAR and L. C. M. MIRANDA, *Phys. Chem. Glasses* **28** (1987) 127.
10. M. J. ADAMS and G. F. KIRKBRIGTH, *Analyst* **102** (1977) 281.
11. R. T. SWIMM, *Appl. Phys. Lett.* **42** (1983) 955.
12. C. L. CESAR, H. VARGAS, J. MENDES-FILHO and L. C. M. MIRANDA, *ibid.* **43** (1983) 555.
13. A. LACHAINE and P. POULET, *ibid.* **45** (1984) 953.
14. O. PESSOA Jr, C. L. CESAR, N. A. PATEL, H. VARGAS, C. C. GHIZONI and L. C. M. MIRANDA, *J. Appl. Phys.* **59** (1986) 1316.
15. M. D. SILVA, I. N. BANDEIRA and L. C. M. MIRANDA, *J. Phys. E. Sci. Instrum.* **20** (1987) 1476.
16. L. F. PERONDI and L. C. M. MIRANDA, *J. Appl. Phys.* **62** (1987) 2955.
17. G. M. SESSLER and J. E. WEST, in "Electrets", in Spring Series in Topics in Applied Physics, Vol. **33**, edited by G. M. Sessler (Springer, Berlin, 1980) p. 347.
18. F. A. McDONALD and G. C. WETSEL Jr, *J. Appl. Phys.* **49** (1978) 2313.
19. A. ROSENCWAIG, in "Photoacoustics and Photoacoustic Spectroscopy" (Wiley, New York, 1980).
20. A. ROSENCWAIG and A. GERSHO, *J. Appl. Phys.* **47** (1976) 64.
21. G. ROUSSET, F. LEPOUTRE and L. BERTRAND, *ibid.* **54** (1983) 2383.
22. J. C. MAXWELL, in "A Treatise on Electricity and Magnetism", 3rd Edn (Oxford University Press, Oxford, 1904) pp. 135-48.
23. L. RAYLEIGH, *Phil. Mag.* **34** (1892) 481.

Received 9 July 1990

and accepted 6 February 1991